

# The one loop corrections to the neutrino masses in BLMSSM

Shu-Min Zhao<sup>1\*</sup>, Tai-Fu Feng<sup>1†</sup>, Xing-Xing Dong<sup>1</sup>,

Hai-Bin Zhang<sup>1</sup>, Guo-Zhu Ning<sup>1</sup>, Tao-Guo<sup>2</sup>

<sup>1</sup> *Department of Physics, Hebei University, Baoding 071002, China*

<sup>2</sup> *School of Mathematics and Science,  
Hebei University of Geosciences, Shijiazhuang 050031, China*

(Dated: September 6, 2021)

## Abstract

The neutrino masses and mixings are studied in the model which is the supersymmetric extension of the standard model with local gauged baryon and lepton numbers(BLMSSM). At tree level the neutrinos can obtain tiny masses through the See-Saw mechanism in the BLMSSM. The one-loop corrections to the neutrino masses and mixings are important, and they are studied in this work with the mass insertion approximation. We study the numerical results and discuss the allowed parameter space of BLMSSM. It can contribute to study the neutrino masses and to explore the new physics beyond the standard model(SM).

PACS numbers: 13.40.Em, 12.60.-i

Keywords: BLMSSM, neutrino mass, mass insertion

---

\* zhaosm@hbu.edu.cn

† fengtf@hbu.edu.cn

## I. INTRODUCTION

When the CP-even Higgs  $h^0$  with  $m_{h^0} = 125.7\text{GeV}$  was detected by LHC in 2012[1], all the particles in SM have been founded. Though SM obtains large successes, it is unable to explain some phenomena. For example, SM can not explain the neutrino masses and their mixing pattern[2], because in SM there are only three left-handed neutrinos with zero mass. The anomalous neutrino data from both solar and atmospheric neutrino experiments promote the study of neutrino masses and lepton flavor violating processes. The authors give out the global analyses of neutrino oscillation experiments in their work, and the present  $3\sigma$  limits for the neutrino experiment data are[3]

$$\begin{aligned}
0.0188 &\leq \sin^2 \theta_{13} \leq 0.0251, \\
0.270 &\leq \sin^2 \theta_{12} \leq 0.344, \\
0.385 &\leq \sin^2 \theta_{23} \leq 0.644, \\
7.02 \times 10^{-5} \text{eV}^2 &\leq \Delta m_{\odot}^2 \leq 8.09 \times 10^{-5} \text{eV}^2, \\
2.325 \times 10^{-3} \text{eV}^2 &\leq \Delta m_A^2(\text{NO}) \leq 2.599 \times 10^{-3} \text{eV}^2, \\
-2.590 \times 10^{-3} \text{eV}^2 &\leq \Delta m_A^2(\text{IO}) \leq -2.307 \times 10^{-3} \text{eV}^2.
\end{aligned} \tag{1}$$

For the mixing pattern, there are two large mixing angles and one small mixing angle. To explain the results in Eq.(1), a theory beyond the SM is necessary. Therefore, the neutrino sector is a natural testing ground for the new models beyond the SM.

For the new physics, the supersymmetric extension of the SM is a popular choice. The discrete symmetry known as  $R$ -parity is defined as  $R_p = (-1)^{L+3B+2S}$  with  $L(B)$ ,  $S$  denoting the lepton (baryon) number and the spin of the particle[4]. The minimal supersymmetric extension of the SM (MSSM)[5] has been studied for many years by theoretical physicists. MSSM with  $R$ -parity conservation has some short comings, where neither  $\mu$  problem nor the observed neutrino masses can be explained.  $R$ -parity violation can be obtained from  $L$  breaking,  $B$  breaking, both  $L$  and  $B$  breaking. In general, to explain the neutrino experiment data, the lepton number should be broken.

In  $R$ -parity violating supersymmetric models with generic soft supersymmetry breaking terms[6], neutrinos and neutralinos mix together at tree level. Therefore, one neutrino gets small mass through the see-saw mechanism[7]. The loop diagrams including lepton number violating effects provide masses to the other neutrinos. Taking into account the one loop

effects, the authors research the neutrino masses and mixings. In  $\mu\nu SSM$  three right-handed neutrino superfields are introduced[8, 9], and it can solve the  $\mu$  problem. In this model[10], the neutrino masses and mixings are studied at one loop level, and significative results are obtained.

The BLMSSM is the minimal supersymmetric extension of the SM with local gauged  $B$  and  $L$ , which is spontaneously broken at TeV scale[11]. This model was first proposed by the authors in Ref.[12]. So BLMSSM is  $R$ -parity violating and can explain the asymmetry of matter-antimatter in the universe. In BLMSSM, the authors study the lightest CP-even Higgs mass and the decays  $h^0 \rightarrow \gamma\gamma$ ,  $h^0 \rightarrow ZZ(WW)$ [13]. The one loop and two loop Barr-Zee type contributions to muon MDM and charged lepton flavor violating processes are also discussed[14]. Considering the CP-violation, we study neutron EDM, lepton EDM and  $B^0 - \bar{B}^0$  mixing in this model[15].

In the BLMSSM, because of the introduced right-handed neutrino fields, the three light neutrinos obtain tiny masses at tree level through the see-saw mechanism, which is shown in our previous work[16]. Here, using the mass insertion approximation we consider one loop corrections to the neutrino mass mixing matrix. The one loop corrections are important, especially for the light neutrinos.

After this introduction, in Section 2 we briefly introduce the BLMSSM. With mass insertion method, the one loop corrections to neutrino mass matrix are shown in Section 3. Section 4 is devoted to the numerical analysis. The summary is given out in Section 5.

## II. SOME CONTENT OF BLMSSM

The gauge symmetry of BLMSSM is  $SU(3)_C \otimes SU(2)_L \otimes U(1)_Y \otimes U(1)_B \otimes U(1)_L$ . Compared with MSSM, BLMSSM includes many new fields[11]:

1. the exotic quarks  $(\hat{Q}_4, \hat{U}_4^c, \hat{D}_4^c, \hat{Q}_5^c, \hat{U}_5, \hat{D}_5)$  used to cancel  $B$  anomaly,
2. the exotic leptons  $(\hat{L}_4, \hat{E}_4^c, \hat{N}_4^c, \hat{L}_5^c, \hat{E}_5, \hat{N}_5)$  used to cancel  $L$  anomaly,
3. the exotic Higgs  $\hat{\Phi}_L, \hat{\varphi}_L$  introduced to break  $L$  spontaneously with nonzero vacuum expectation values (VEVs),
4. the exotic Higgs  $\hat{\Phi}_B, \hat{\varphi}_B$  introduced to break  $B$  spontaneously with nonzero VEVs,
5. the superfields  $\hat{X}$  and  $\hat{X}'$  used to make the exotic quarks unstable,
6. the right-handed neutrinos  $N_R^c$  introduced to provide tiny masses of neutrinos through

see-saw mechanism.

The lightest mass eigenstate of the mixed mass matrix for  $\hat{X}$  and  $\hat{X}'$  could be a dark matter candidate. These new fields are shown particularly in the table1.

TABLE I: The new fields in the BLMSSM: the exotic quarks, exotic leptons, exotic Higgs,  $X$  superfields and right-handed neutrinos.

Superfields	$SU(3)_C$	$SU(2)_L$	$U(1)_Y$	$U(1)_B$	$U(1)_L$
$\hat{Q}_4$	3	2	1/6	$B_4$	0
$\hat{U}_4^c$	$\bar{3}$	1	-2/3	$-B_4$	0
$\hat{D}_4^c$	$\bar{3}$	1	1/3	$-B_4$	0
$\hat{Q}_5^c$	$\bar{3}$	2	-1/6	$-(1 + B_4)$	0
$\hat{U}_5$	3	1	2/3	$1 + B_4$	0
$\hat{D}_5$	3	1	-1/3	$1 + B_4$	0
$\hat{L}_4$	1	2	-1/2	0	$L_4$
$\hat{E}_4^c$	1	1	1	0	$-L_4$
$\hat{N}_4^c$	1	1	0	0	$-L_4$
$\hat{L}_5^c$	1	2	1/2	0	$-(3 + L_4)$
$\hat{E}_5$	1	1	-1	0	$3 + L_4$
$\hat{N}_5$	1	1	0	0	$3 + L_4$
$\hat{\Phi}_B$	1	1	0	1	0
$\hat{\varphi}_B$	1	1	0	-1	0
$\hat{\Phi}_L$	1	1	0	0	-2
$\hat{\varphi}_L$	1	1	0	0	2
$\hat{X}$	1	1	0	$2/3 + B_4$	0
$\hat{X}'$	1	1	0	$-(2/3 + B_4)$	0
$\hat{N}_R^c$	1	1	0	0	-1

The superpotential of BLMSSM is written as [11, 13]

$$\mathcal{W}_{BLMSSM} = \mathcal{W}_{MSSM} + \mathcal{W}_B + \mathcal{W}_L + \mathcal{W}_X , \quad (2)$$

with  $\mathcal{W}_{MSSM}$  denoting the superpotential of the MSSM. The concrete forms of  $\mathcal{W}_B, \mathcal{W}_L$  and  $\mathcal{W}_X$  are

$$\begin{aligned}
\mathcal{W}_B &= \lambda_Q \hat{Q}_4 \hat{Q}_5^c \hat{\Phi}_B + \lambda_U \hat{U}_4 \hat{U}_5 \hat{\varphi}_B + \lambda_D \hat{D}_4^c \hat{D}_5 \hat{\varphi}_B + \mu_B \hat{\Phi}_B \hat{\varphi}_B \\
&\quad + Y_{u_4} \hat{Q}_4 \hat{H}_u \hat{U}_4^c + Y_{d_4} \hat{Q}_4 \hat{H}_d \hat{D}_4^c + Y_{u_5} \hat{Q}_5^c \hat{H}_d \hat{U}_5 + Y_{d_5} \hat{Q}_5^c \hat{H}_u \hat{D}_5, \\
\mathcal{W}_L &= Y_{e_4} \hat{L}_4 \hat{H}_d \hat{E}_4^c + Y_{\nu_4} \hat{L}_4 \hat{H}_u \hat{N}_4^c + Y_{e_5} \hat{L}_5^c \hat{H}_u \hat{E}_5 + Y_{\nu_5} \hat{L}_5^c \hat{H}_d \hat{N}_5 \\
&\quad + Y_\nu \hat{L} \hat{H}_u \hat{N}^c + \lambda_{N^c} \hat{N}^c \hat{N}^c \hat{\varphi}_L + \mu_L \hat{\Phi}_L \hat{\varphi}_L, \\
\mathcal{W}_X &= \lambda_1 \hat{Q} \hat{Q}_5^c \hat{X} + \lambda_2 \hat{U} \hat{U}_5 \hat{X}' + \lambda_3 \hat{D}^c \hat{D}_5 \hat{X}' + \mu_X \hat{X} \hat{X}'. \tag{3}
\end{aligned}$$

The soft breaking terms  $\mathcal{L}_{soft}$  of the BLMSSM can be found in the works[11–13].

$$\begin{aligned}
\mathcal{L}_{soft} &= \mathcal{L}_{soft}^{MSSM} - (m_{\tilde{\nu}^c}^2)_{IJ} \tilde{N}_I^{c*} \tilde{N}_J^c - m_{\tilde{Q}_4}^2 \tilde{Q}_4^\dagger \tilde{Q}_4 - m_{\tilde{U}_4}^2 \tilde{U}_4^{c*} \tilde{U}_4^c - m_{\tilde{D}_4}^2 \tilde{D}_4^{c*} \tilde{D}_4^c \\
&\quad - m_{\tilde{Q}_5}^2 \tilde{Q}_5^{c\dagger} \tilde{Q}_5^c - m_{\tilde{U}_5}^2 \tilde{U}_5^{c*} \tilde{U}_5^c - m_{\tilde{D}_5}^2 \tilde{D}_5^{c*} \tilde{D}_5^c - m_{\tilde{L}_4}^2 \tilde{L}_4^\dagger \tilde{L}_4 - m_{\tilde{\nu}_4}^2 \tilde{N}_4^{c*} \tilde{N}_4^c \\
&\quad - m_{\tilde{e}_4}^2 \tilde{E}_4^{c*} \tilde{E}_4^c - m_{\tilde{L}_5}^2 \tilde{L}_5^{c\dagger} \tilde{L}_5^c - m_{\tilde{\nu}_5}^2 \tilde{N}_5^{c*} \tilde{N}_5^c - m_{\tilde{e}_5}^2 \tilde{E}_5^{c*} \tilde{E}_5^c - m_{\Phi_B}^2 \Phi_B^* \Phi_B \\
&\quad - m_{\varphi_B}^2 \varphi_B^* \varphi_B - m_{\Phi_L}^2 \Phi_L^* \Phi_L - m_{\varphi_L}^2 \varphi_L^* \varphi_L - (m_B \lambda_B \lambda_B + m_L \lambda_L \lambda_L + h.c.) \\
&\quad + \{ A_{u_4} Y_{u_4} \tilde{Q}_4 H_u \tilde{U}_4^c + A_{d_4} Y_{d_4} \tilde{Q}_4 H_d \tilde{D}_4^c + A_{u_5} Y_{u_5} \tilde{Q}_5^c H_d \tilde{U}_5 + A_{d_5} Y_{d_5} \tilde{Q}_5^c H_u \tilde{D}_5 \\
&\quad + A_{BQ} \lambda_Q \tilde{Q}_4 \tilde{Q}_5^c \Phi_B + A_{BU} \lambda_U \tilde{U}_4^c \tilde{U}_5 \varphi_B + A_{BD} \lambda_D \tilde{D}_4^c \tilde{D}_5 \varphi_B + B_B \mu_B \Phi_B \varphi_B + h.c. \} \\
&\quad + \{ A_{e_4} Y_{e_4} \tilde{L}_4 H_d \tilde{E}_4^c + A_{\nu_4} Y_{\nu_4} \tilde{L}_4 H_u \tilde{N}_4^c + A_{e_5} Y_{e_5} \tilde{L}_5^c H_u \tilde{E}_5 + A_{\nu_5} Y_{\nu_5} \tilde{L}_5^c H_d \tilde{N}_5 \\
&\quad + A_{N^c} Y_{\nu} \tilde{L} H_u \tilde{N}^c + A_{N^c} \lambda_{N^c} \tilde{N}^c \tilde{N}^c \varphi_L + B_L \mu_L \Phi_L \varphi_L + h.c. \} \\
&\quad + \{ A_1 \lambda_1 \tilde{Q} \tilde{Q}_5^c X + A_2 \lambda_2 \tilde{U} \tilde{U}_5 X' + A_3 \lambda_3 \tilde{D}^c \tilde{D}_5 X' + B_X \mu_X X X' + h.c. \}, \tag{4}
\end{aligned}$$

When the Higgs fields including  $SU(2)_L$  doublets  $(H_u, H_d)$  and  $SU(2)_L$  singlets  $(\Phi_L, \varphi_L, \Phi_B, \varphi_B)$  obtain nonzero VEVs, the local gauge symmetry  $SU(2)_L \otimes U(1)_Y \otimes U(1)_B \otimes U(1)_L$  breaks down to the electromagnetic symmetry  $U(1)_e$ . The  $SU(2)_L$  doublets  $H_u, H_d$  are defined as

$$H_u = \begin{pmatrix} H_u^+ \\ \frac{1}{\sqrt{2}}(v_u + H_u^0 + iP_u^0) \end{pmatrix}, \quad H_d = \begin{pmatrix} \frac{1}{\sqrt{2}}(v_d + H_d^0 + iP_d^0) \\ H_d^- \end{pmatrix}, \tag{5}$$

with nonzero VEVs  $v_u, v_d$ . The  $SU(2)_L$  singlets  $(\Phi_B, \varphi_B, \Phi_L, \varphi_L)$  have nonzero VEVs  $v_B, \bar{v}_B, v_L, \bar{v}_L$ .

$$\begin{aligned}
\Phi_B &= \frac{1}{\sqrt{2}}(v_B + \Phi_B^0 + iP_B^0), & \varphi_B &= \frac{1}{\sqrt{2}}(\bar{v}_B + \varphi_B^0 + i\bar{P}_B^0), \\
\Phi_L &= \frac{1}{\sqrt{2}}(v_L + \Phi_L^0 + iP_L^0), & \varphi_L &= \frac{1}{\sqrt{2}}(\bar{v}_L + \varphi_L^0 + i\bar{P}_L^0). \tag{6}
\end{aligned}$$

### III. THE COUPLING

Because in the BLMSSM neutrinos are Majorana particles, we can use the following expressions for the neutrinos. In the base  $(\psi_{\nu_L}^I, \psi_{N_R^{cI}})$ , the formulae for mass mixing matrix and mass eigenstates are shown here[15].

$$Z_{N_\nu}^T \begin{pmatrix} 0 & \frac{v_u}{\sqrt{2}}(Y_\nu)^{IJ} \\ \frac{v_u}{\sqrt{2}}(Y_\nu^T)^{IJ} & \frac{\bar{v}_L}{\sqrt{2}}(\lambda_{N^c})^{IJ} \end{pmatrix} Z_{N_\nu} = \text{diag}(m_{\nu^\alpha}), \quad \alpha = 1 \dots 6, \quad I, J = 1, 2, 3,$$

$$\psi_{\nu_L}^I = Z_{N_\nu}^{I\alpha} k_{N_\alpha}^0, \quad \psi_{N_R^{cI}} = Z_{N_\nu}^{(I+3)\alpha} \bar{k}_{N_\alpha}^0, \quad \chi_{N_\alpha}^0 = \begin{pmatrix} k_{N_\alpha}^0 \\ \bar{k}_{N_\alpha}^0 \end{pmatrix}. \quad (7)$$

$\chi_{N_\alpha}^0 (\alpha = 1 \dots 6)$  denote the mass eigenstates of the neutrino fields mixed by left-handed and right-handed neutrinos.

The exotic gauginos  $(\lambda_L, \lambda_B)$  and exotic Higgs super fields  $(\psi_{\Phi_L}, \psi_{\varphi_L}, \psi_{\Phi_B}, \psi_{\varphi_B})$  are introduced in BLMSSM. They mix together leading to six new neutralinos beyond MSSM. However, the six new neutralinos do not mix with the four MSSM neutralinos.  $\lambda_L$  (the superpartners of the new lepton boson) and  $\psi_{\Phi_L}, \psi_{\varphi_L}$  (the superpartners of the  $SU(2)_L$  singlets  $\Phi_L, \varphi_L$ ) mix and they produce three lepton neutralinos. In the basis  $(i\lambda_L, \psi_{\Phi_L}, \psi_{\varphi_L})$ , the mass mixing matrix of lepton neutralinos is[15]

$$\begin{pmatrix} 2M_L & 2v_L g_L & -2\bar{v}_L g_L \\ 2v_L g_L & 0 & -\mu_L \\ -2\bar{v}_L g_L & -\mu_L & 0 \end{pmatrix}. \quad (8)$$

To get the mass eigenstates for lepton neutralinos, we use the rotation matrix  $Z_{N_L}$  to diagonalize the mass mixing matrix in Eq.(8).

Similarly, three baryon neutralinos are produced from  $\lambda_B$  (the superpartners of the new baryon boson) and  $\psi_{\Phi_B}, \psi_{\varphi_B}$  (the superpartners of the  $SU(2)_L$  singlets  $\Phi_B, \varphi_B$ ). We show the mass mixing matrix of baryon neutralinos here in the basis  $(i\lambda_B, \psi_{\Phi_B}, \psi_{\varphi_B})$

$$\begin{pmatrix} 2M_B & 2v_B g_B & -2\bar{v}_B g_B \\ 2v_B g_B & 0 & -\mu_B \\ -2\bar{v}_B g_B & -\mu_B & 0 \end{pmatrix}. \quad (9)$$

To obtain three baryon neutrino masses, we use the rotation matrix  $Z_{N_B}$  to diagonalize the mass mixing matrix in Eq.(9).

From the superpotential  $\mathcal{W}_L$  and the interactions of gauge and matter multiplets  $ig\sqrt{2}T_{ij}^a(\lambda^a\psi_jA_i^* - \bar{\lambda}^a\bar{\psi}_iA_j)$ , we obtain the couplings with light neutrinos at tree level.

$$\begin{aligned}\mathcal{L}_L(\nu) = & -Y_l^{IJ}Z_-^{2i}Z_{N_\nu}^{I\alpha}\bar{\chi}_i^+\omega_-\chi_{N_\alpha}^0\tilde{e}_R^{JC} - Y_\nu^{IJ}Z_N^{4i}Z_{N_\nu}^{I\alpha}\bar{\chi}_i^0\omega_-\chi_{N_\alpha}^0\tilde{N}_R^{cJ} \\ & -Y_l^{IJ}Z_{N_\nu}^{I\alpha}\bar{e}^J\omega_-\chi_{N_\alpha}^0H_d^2 - Y_\nu^{IJ}Z_{N_\nu}^{I\alpha}Z_{N_\nu}^{(3+J)\beta}\bar{\chi}_{N_\beta}^0\omega_-\chi_{N_\alpha}^0H_u^2 \\ & -g_2Z_-^{1i}Z_{N_\nu}^{I\alpha}\bar{\chi}_i^+\omega_-\chi_{N_\alpha}^0\tilde{e}_L^{*-} + \sqrt{2}g_LZ_{N_L}^{1i}Z_{N_\nu}^{I\alpha}\bar{\chi}_{Li}^0\omega_-\chi_{N_\alpha}^0\tilde{\nu}_L^* \\ & -\frac{1}{\sqrt{2}}Z_{N_\nu}^{I\alpha}(g_2Z_N^{2i} - g_1Z_N^{1i})\bar{\chi}_i^0\omega_-\chi_{N_\alpha}^0\tilde{\nu}_L^{I*} + h.c.\end{aligned}\quad (10)$$

In the same way, the couplings related to heavy neutrinos are also obtained

$$\begin{aligned}\mathcal{L}_H(\nu) = & Y_\nu^{IJ}Z_{N_\nu}^{(J+3)\alpha}\bar{\chi}_{N_\alpha}^0\omega_-e^IH_u^1 + Y_\nu^{IJ}Z_+^{2i}Z_{N_\nu}^{(J+3)\alpha}\bar{\chi}_{N_\alpha}^0\omega_-\chi_i^+\tilde{e}_L^I \\ & -Y_\nu^{IJ}Z_N^{4i}Z_{N_\nu}^{(J+3)\alpha}\bar{\chi}_{N_\alpha}^0\omega_-\chi_i^0\tilde{\nu}_L^I - \lambda_{N^c}^{IJ}Z_{N_\nu}^{(I+3)\alpha}Z_{N_\nu}^{(J+3)\beta}\bar{\chi}_{N_\alpha}^0\omega_-\chi_{N_\beta}^0\varphi_L \\ & -\left((\lambda_{N^c}^{IJ} + \lambda_{N^c}^{JI})Z_{N_L}^{3i} + \sqrt{2}g_LZ_{N_L}^{1i}\delta^{IJ}\right)Z_{N_\nu}^{(I+3)\alpha}\bar{\chi}_{N_\alpha}^0\omega_-\chi_{Li}^0N_R^{cJ} + h.c.\end{aligned}\quad (11)$$

#### IV. THE ONE LOOP CORRECTIONS TO NEUTRINO MASS MATRIX

The neutrino Yukawa couplings  $(Y_\nu)^{IJ}$ ,  $(I, J = 1, 2, 3)$  are much smaller than the other couplings. For Eqs.(10)(11), the terms  $-Y_\nu^{IJ}Z_N^{4i}Z_{N_\nu}^{I\alpha}\bar{\chi}_i^0\omega_-\chi_{N_\alpha}^0\tilde{N}_R^{cJ} - Y_\nu^{IJ}Z_{N_\nu}^{I\alpha}Z_{N_\nu}^{(3+J)\beta}\bar{\chi}_{N_\beta}^0\omega_-\chi_{N_\alpha}^0H_u^2$  in  $\mathcal{L}_L(\nu)$ , and  $Y_\nu^{IJ}Z_{N_\nu}^{(J+3)\alpha}\bar{\chi}_{N_\alpha}^0\omega_-e^IH_u^1 + Y_\nu^{IJ}Z_+^{2i}Z_{N_\nu}^{(J+3)\alpha}\bar{\chi}_{N_\alpha}^0\omega_-\chi_i^+\tilde{e}_L^I - Y_\nu^{IJ}Z_N^{4i}Z_{N_\nu}^{(J+3)\alpha}\bar{\chi}_{N_\alpha}^0\omega_-\chi_i^0\tilde{\nu}_L^I$  in  $\mathcal{L}_H(\nu)$  can be neglected safely, because they are suppressed by  $Y_\nu$  compared with the other terms. The  $Y_\nu$  in the neutrino mass mixing matrix at tree level is not neglected. One can find that  $Z_{N_\nu}$  is the function of  $Y_\nu$  from Eq.(7). That is to say,  $Z_{N_\nu}$  is relevant to the chiral symmetry breaking terms.

Using the mass insertion approximation[17], we deduce the neutrino mass corrections from the virtual slepton-chargino at one loop level

$$\begin{aligned}\delta(m_\nu)_{\alpha\theta}(\tilde{e}_L, \tilde{e}_R, \chi_i^\pm) = & \frac{m_{\chi_i^\pm}}{\Lambda^2}\left(Z_{N_\nu}^{I\alpha}Z_{N_\nu}^{J\theta}Y_l^IY_l^J(Z_-^{2i})^2\delta(M_{\tilde{L}}^2)_{RR}^{IJ}I_{111}^0(x_{\chi_i^\pm}, x_{\tilde{e}_R^K}, x_{\tilde{e}_R^I}) \right. \\ & + (Z_{N_\nu}^{I\theta}Z_{N_\nu}^{J\alpha} + Z_{N_\nu}^{I\alpha}Z_{N_\nu}^{J\theta})g_2Y_l^IY_l^JZ_-^{1i}Z_-^{2i}\delta(M_{\tilde{L}}^2)_{RL}^{IJ}I_{111}^0(x_{\chi_i^\pm}, x_{\tilde{e}_R^I}, x_{\tilde{e}_L^J}) \\ & \left. + Z_{N_\nu}^{I\alpha}Z_{N_\nu}^{J\theta}g_2^2(Z_-^{1i})^2\delta(M_{\tilde{L}}^2)_{LL}^{IJ}I_{111}^0(x_{\chi_i^\pm}, x_{\tilde{e}_L^I}, x_{\tilde{e}_L^J})\right).\end{aligned}\quad (12)$$

The one loop function  $I_{111}^0(x_1, x_2, x_3)$  is defined from the following formula

$$i \int \frac{dk^4}{(2\pi)^4} \frac{1}{k^2 - m_1^2} \frac{1}{k^2 - m_2^2} \frac{1}{k^2 - m_3^2} = \frac{1}{\Lambda^2} I_{111}^0(x_1, x_2, x_3), \quad (13)$$

with  $\Lambda$  representing the energy scale of the new physics and  $x_i = \frac{m_i^2}{\Lambda^2}$  for  $i = 1, 2, 3$ . In Eq.(12), it seems that the results have nothing to do with the chiral symmetry breaking terms. In fact, Eq.(12) includes  $Z_{N_\nu}$  which is the function of nonzero  $Y_\nu$ . Therefore, Eq.(12) includes the chiral symmetry breaking terms and gives corrections to the neutrino mass mixing matrix.

In the same way, the neutrino mass corrections from the virtual sneutrino-lepton neutralino and sneutrino-neutralino are obtained

$$\begin{aligned} \delta(m_\nu)_{\alpha\theta}(\tilde{\nu}_L, \tilde{N}_R^c, \chi_{L_i}^0) &= \frac{m_{\chi_{L_i}^0}}{\Lambda^2} \left( 2g_L^2 (Z_{N_L}^{1i})^2 Z_{N_\nu}^{I\alpha} Z_{N_\nu}^{J\theta} \delta(M_\nu^2)_{LL}^{IJ} I_{111}^0(x_{\chi_{L_i}^0}, x_{\tilde{\nu}_L^I}, x_{\tilde{\nu}_L^J}) \right. \\ &\quad - \sqrt{2}g_L Z_{N_L}^{1i} (Z_{N_\nu}^{I\alpha} Z_{N_\nu}^{(K+3)\theta} + Z_{N_\nu}^{I\theta} Z_{N_\nu}^{(K+3)\alpha}) \delta(M_\nu^2)_{LR}^{IJ} [(\lambda_{N^c}^{KJ} + \lambda_{N^c}^{JK}) Z_{N_L}^{3i} + \sqrt{2}g_L Z_{N_L}^{1i} \delta^{KJ}] \\ &\quad \times I_{111}^0(x_{\chi_{L_i}^0}, x_{\tilde{\nu}_L^I}, x_{\tilde{N}_R^{cJ}}) + Z_{N_\nu}^{(I+3)\theta} Z_{N_\nu}^{(F+3)\alpha} \delta(M_\nu^2)_{RR}^{KJ} [(\lambda_{N^c}^{IJ} + \lambda_{N^c}^{JI}) Z_{N_L}^{3i} + \sqrt{2}g_L Z_{N_L}^{1i} \delta^{IJ}] \\ &\quad \times [(\lambda_{N^c}^{FK} + \lambda_{N^c}^{KF}) Z_{N_L}^{3i} + \sqrt{2}g_L Z_{N_L}^{1i} \delta^{KF}] I_{111}^0(x_{\chi_{L_i}^0}, x_{\tilde{N}_R^{cK}}, x_{\tilde{N}_R^{cJ}}) \Big), \\ \delta(m_\nu)_{\alpha\theta}(\tilde{\nu}_L, \chi_i^0) &= \frac{1}{2\Lambda^2} Z_{N_\nu}^{I\alpha} Z_{N_\nu}^{J\theta} (g_2 Z_N^{2i} - g_1 Z_N^{1i})^2 m_{\chi_i^0} \delta(M_\nu^2)_{LL}^{IJ} I_{111}^0(x_{\chi_i^0}, x_{\tilde{\nu}_L^I}, x_{\tilde{\nu}_L^J}). \end{aligned} \quad (14)$$

The virtual Higgs-charged lepton and exotic Higgs-neutrino can also give the contributions

$$\begin{aligned} \delta(m_\nu)_{\alpha\theta}(H_d^2, e^I) &= \frac{m_{e^I}}{\Lambda^2} Y_l^I Y_l^I Z_{N_\nu}^{I\alpha} Z_{N_\nu}^{I\theta} \delta(M^2)_{H_d^2 H_d^2} I_{12}^0(x_{e^I}, x_{H_d^2}), \\ \delta(m_\nu)_{\alpha\theta}(\varphi_L^0, \bar{P}_L^0, \chi_{N_\nu}) &= \frac{m_{\chi_\nu^0}}{2\Lambda^2} \lambda_{N^c}^{IJ} \lambda_{N^c}^{JK} Z_{N_\nu}^{(I+3)\theta} Z_{N_\nu}^{(K+3)\alpha} (Z_{N_\nu}^{(J+3)\beta})^2 \\ &\quad \times \left( \delta(M_{\varphi_L^0 \varphi_L^0}^2) I_{12}^0(x_{\chi_\nu^0}, x_{\varphi_L^0}), + \delta(M_{\bar{P}_L^0 \bar{P}_L^0}^2) I_{12}^0(x_{\chi_\nu^0}, x_{\bar{P}_L^0}) \right). \end{aligned} \quad (15)$$

The definition of  $I_{12}^0(x_1, x_2)$  is

$$i \int \frac{dk^4}{(2\pi)^4} \frac{1}{k^2 - m_1^2} \frac{1}{(k^2 - m_2^2)^2} = \frac{1}{\Lambda^2} I_{12}^0(x_1, x_2). \quad (16)$$

In the flavor basis at tree level the neutrino mass mixing matrix is

$$M_N = \begin{pmatrix} 0 & \frac{v_u}{\sqrt{2}} (Y_\nu)^{IJ} \\ \frac{v_u}{\sqrt{2}} (Y_\nu^T)^{IJ} & \frac{\bar{v}_L}{\sqrt{2}} (\lambda_{N^c})^{IJ} \end{pmatrix}. \quad (17)$$

With the rotation matrix  $Z_{N_\nu}$ , the masses of neutrinos are gotten by the formula  $Z_{N_\nu}^T M_N Z_{N_\nu} = \text{diag}(m_{\nu^\alpha})$ ,  $\alpha = 1 \dots 6$ . We use the matrix  $Z_{N_\nu}^T$  in the leading order of  $\varsigma$ , which is defined as  $\varsigma = \frac{v_u}{\bar{v}_L} (Y_\nu)_{3 \times 3} \cdot (\lambda_{N^c})_{3 \times 3}^{-1}$ . All the elements in  $\varsigma$  are very small ( $\varsigma_{IJ} \ll 1$ ), because they are suppressed by the tiny neutrino Yukawa  $Y_\nu$ . It is a good approximation to adopt  $Z_{N_\nu}^T$  in the following form[10]

$$Z_{N_\nu}^T = \begin{pmatrix} \mathcal{S}^T & 0 \\ 0 & \mathcal{R}^T \end{pmatrix} \cdot \begin{pmatrix} 1 - \frac{1}{2} \varsigma^\dagger \varsigma & -\varsigma^\dagger \\ \varsigma & 1 - \frac{1}{2} \varsigma \varsigma^\dagger \end{pmatrix}. \quad (18)$$



We use the matrices  $\mathcal{S}$  and  $\mathcal{R}$  defined in Eq.(18) to diagonalize  $M_\nu^{seesaw}$  and  $\frac{\bar{v}_L}{\sqrt{2}}\lambda_{N^c}$

$$\begin{aligned}\mathcal{S}^T M_\nu^{seesaw} \mathcal{S} &= \text{diag}(m_{\nu_1}, m_{\nu_2}, m_{\nu_3}), \\ \mathcal{R}^T \frac{\bar{v}_L}{\sqrt{2}} (\lambda_{N^c})^{IJ} \mathcal{R} &= \text{diag}(m_{\nu_4}, m_{\nu_5}, m_{\nu_6}).\end{aligned}\quad (19)$$

In this condition,  $M_\nu^{seesaw}$  is expressed as

$$M_\nu^{seesaw} = -\frac{v_u^2}{\bar{v}_L} (Y_\nu)_{3 \times 3} (\lambda_{N^c})_{3 \times 3}^{-1} (Y_\nu^T)_{3 \times 3}. \quad (20)$$

The one loop corrections are calculated in the mass basis at tree level, which is  $(\psi_{\nu_L^I}, \psi_{N_R^{cI}}) Z_{N_\nu}$ . Here, we obtain the sum of one loop corrections from Eqs.(12,14,15)

$$\begin{aligned}\Delta(M_N)_{\alpha\theta} &= \delta(m_\nu)_{\alpha\theta}(\tilde{e}_L, \tilde{e}_R, \chi_i^\pm) + \delta(m_\nu)_{\alpha\theta}(\tilde{\nu}_L, \chi_i^0) + \delta(m_\nu)_{\alpha\theta}(H_d^2, e^I) \\ &\quad + \delta(m_\nu)_{\alpha\theta}(\tilde{\nu}_L, \tilde{N}_R^c, \chi_{L_i}^0) + \delta(m_\nu)_{\alpha\theta}(\varphi_L^0, \bar{P}_L^0, \chi_{N_\nu}).\end{aligned}\quad (21)$$

For neutrino mass mixing matrix, to get the sum of tree level results and one loop level corrections, we rotate  $\Delta M_N$  into the flavor basis  $(\psi_{\nu_L^I}, \psi_{N_R^{cI}})$ . Therefore the sum can be expressed as

$$\begin{aligned}M_N^{sum} &= M_N + Z_{N_\nu} \Delta M_N Z_{N_\nu}^T \\ &= \begin{pmatrix} \Delta(m_{\nu\nu}) & \frac{v_u}{\sqrt{2}} Y_\nu + \Delta(m_{\nu N^c}) \\ (\frac{v_u}{\sqrt{2}} Y_\nu + \Delta(m_{\nu N^c}))^T & \frac{\bar{v}_L}{\sqrt{2}} \lambda_{N^c} + \Delta(m_{N^c N^c}) \end{pmatrix}.\end{aligned}\quad (22)$$

Obviously, the matrix  $M_N^{sum}$  in Eq.(22) including the one loop corrections also possesses a seesaw structure. Similar as Eq.(20), at one loop level we obtain the corrected effective light neutrino mass matrix in the following form[10]

$$\mathcal{M}_\nu^{eff} \approx \Delta(m_{\nu\nu}) - \left( \frac{v_u Y_\nu}{\sqrt{2}} + \Delta(m_{\nu N^c}) \right) \left( \frac{\bar{v}_L \lambda_{N^c}}{\sqrt{2}} + \Delta(m_{N^c N^c}) \right)^{-1} \left( \frac{v_u Y_\nu}{\sqrt{2}} + \Delta(m_{\nu N^c}) \right)^T. \quad (23)$$

Using the " top-down " method[18], from the one loop corrected effective light neutrino mass matrix  $\mathcal{M}_\nu^{eff}$  we get the Hermitian matrix

$$\mathcal{H} = (\mathcal{M}_\nu^{eff})^\dagger \mathcal{M}_\nu^{eff}. \quad (24)$$

One can diagonalize the  $3 \times 3$  matrix  $\mathcal{H}$  to gain three eigenvalues

$$\begin{aligned}m_1^2 &= \frac{a}{3} - \frac{1}{3}p(\cos \phi + \sqrt{3} \sin \phi), \\ m_2^2 &= \frac{a}{3} - \frac{1}{3}p(\cos \phi - \sqrt{3} \sin \phi), \\ m_3^2 &= \frac{a}{3} + \frac{2}{3}p \cos \phi.\end{aligned}\quad (25)$$

The concrete forms of the parameters in Eq.(25) are collected here

$$\begin{aligned} p &= \sqrt{a^2 - 3b}, \quad \phi = \frac{1}{3} \arccos\left(\frac{1}{p^3}\left(a^3 - \frac{9}{2}ab + \frac{27}{2}c\right)\right), \quad a = \text{Tr}(\mathcal{H}), \\ b &= \mathcal{H}_{11}\mathcal{H}_{22} + \mathcal{H}_{11}\mathcal{H}_{33} + \mathcal{H}_{22}\mathcal{H}_{33} - \mathcal{H}_{12}^2 - \mathcal{H}_{13}^2 - \mathcal{H}_{23}^2, \quad c = \text{Det}(\mathcal{H}). \end{aligned} \quad (26)$$

For the neutrino mass spectrum, there are two possibilities in the 3-neutrino mixing case.

The neutrino mass spectrum with normal ordering (NO) is

$$\begin{aligned} m_{\nu_1} &< m_{\nu_2} < m_{\nu_3}, \quad m_{\nu_1}^2 = m_1^2, \quad m_{\nu_2}^2 = m_2^2, \quad m_{\nu_3}^2 = m_3^2, \\ \Delta m_{\odot}^2 &= m_{\nu_2}^2 - m_{\nu_1}^2 = \frac{2}{\sqrt{3}}p \sin \phi > 0, \\ \Delta m_A^2 &= m_{\nu_3}^2 - m_{\nu_1}^2 = p(\cos \phi + \frac{1}{\sqrt{3}} \sin \phi) > 0. \end{aligned} \quad (27)$$

We also write down the neutrino mass spectrum with inverted ordering (IO)

$$\begin{aligned} m_{\nu_3} &< m_{\nu_1} < m_{\nu_2}, \quad m_{\nu_3}^2 = m_1^2, \quad m_{\nu_1}^2 = m_2^2, \quad m_{\nu_2}^2 = m_3^2, \\ \Delta m_{\odot}^2 &= m_{\nu_2}^2 - m_{\nu_1}^2 = p(\cos \phi - \frac{1}{\sqrt{3}} \sin \phi) > 0, \\ \Delta m_A^2 &= m_{\nu_3}^2 - m_{\nu_2}^2 = -p(\cos \phi + \frac{1}{\sqrt{3}} \sin \phi) < 0. \end{aligned} \quad (28)$$

From the mass squared matrix  $\mathcal{H}$ , one gets the normalized eigenvectors

$$\begin{aligned} \begin{pmatrix} (U_\nu)_{11} \\ (U_\nu)_{21} \\ (U_\nu)_{31} \end{pmatrix} &= \frac{1}{\sqrt{|X_1|^2 + |Y_1|^2 + |Z_1|^2}} \begin{pmatrix} X_1 \\ Y_1 \\ Z_1 \end{pmatrix}, \\ \begin{pmatrix} (U_\nu)_{12} \\ (U_\nu)_{22} \\ (U_\nu)_{32} \end{pmatrix} &= \frac{1}{\sqrt{|X_2|^2 + |Y_2|^2 + |Z_2|^2}} \begin{pmatrix} X_2 \\ Y_2 \\ Z_2 \end{pmatrix}, \\ \begin{pmatrix} (U_\nu)_{13} \\ (U_\nu)_{23} \\ (U_\nu)_{33} \end{pmatrix} &= \frac{1}{\sqrt{|X_3|^2 + |Y_3|^2 + |Z_3|^2}} \begin{pmatrix} X_3 \\ Y_3 \\ Z_3 \end{pmatrix}. \end{aligned} \quad (29)$$

The concrete forms of  $X_I, Y_I, Z_I$  for  $I = 1, 2, 3$  are shown here

$$\begin{aligned} X_1 &= (\mathcal{H}_{22} - m_{\nu_1}^2)(\mathcal{H}_{33} - m_{\nu_1}^2) - \mathcal{H}_{23}^2, & Y_1 &= \mathcal{H}_{13}\mathcal{H}_{23} - \mathcal{H}_{12}(\mathcal{H}_{33} - m_{\nu_1}^2), \\ Z_1 &= \mathcal{H}_{12}\mathcal{H}_{23} - \mathcal{H}_{13}(\mathcal{H}_{22} - m_{\nu_1}^2), & X_2 &= \mathcal{H}_{13}\mathcal{H}_{23} - \mathcal{H}_{12}(\mathcal{H}_{33} - m_{\nu_2}^2), \\ Y_2 &= (\mathcal{H}_{11} - m_{\nu_2}^2)(\mathcal{H}_{33} - m_{\nu_2}^2) - \mathcal{H}_{13}^2, & Z_2 &= \mathcal{H}_{12}\mathcal{H}_{13} - \mathcal{H}_{23}(\mathcal{H}_{11} - m_{\nu_2}^2), \\ X_3 &= \mathcal{H}_{12}\mathcal{H}_{23} - \mathcal{H}_{13}(\mathcal{H}_{22} - m_{\nu_3}^2), & Y_3 &= \mathcal{H}_{12}\mathcal{H}_{13} - \mathcal{H}_{23}(\mathcal{H}_{11} - m_{\nu_3}^2), \\ Z_3 &= (\mathcal{H}_{11} - m_{\nu_3}^2)(\mathcal{H}_{22} - m_{\nu_3}^2) - \mathcal{H}_{12}^2. \end{aligned} \quad (30)$$

The mixing angles among three tiny neutrinos can be defined as follows

$$\begin{aligned}
\sin \theta_{13} &= |(U_\nu)_{13}|, & \cos \theta_{13} &= \sqrt{1 - |(U_\nu)_{13}|^2}, \\
\sin \theta_{23} &= \frac{|(U_\nu)_{23}|}{\sqrt{1 - |(U_\nu)_{13}|^2}}, & \cos \theta_{23} &= \frac{|(U_\nu)_{33}|}{\sqrt{1 - |(U_\nu)_{13}|^2}}, \\
\sin \theta_{12} &= \frac{|(U_\nu)_{12}|}{\sqrt{1 - |(U_\nu)_{13}|^2}}, & \cos \theta_{12} &= \frac{|(U_\nu)_{11}|}{\sqrt{1 - |(U_\nu)_{13}|^2}}.
\end{aligned} \tag{31}$$

## V. NUMERICAL RESULTS

In this section, we discuss the numerical results for the neutrinos including three mixing angles and two mass squared differences. Using BLMSSM, we have studied several processes in our precious works, such as the lightest neutral CP-even Higgs mass and the charged lepton flavor violating processes. Because the masses of light neutrinos are very tiny at  $10^{-1}$  TeV order, the used parameters should be precise enough. In this work, the tiny neutrino Yukawa  $Y_\nu$  can give contributions to light neutrino masses at tree level through the see-saw mechanism. Therefore,  $Y_\nu$  are important parameters and should be considered earnestly.

We show the used parameters

$$\begin{aligned}
B_H &= 800\text{GeV}, \quad \mu_H = 650\text{GeV}, \quad m_1 = -1\text{TeV}, \quad m_2 = -500\text{GeV}, \quad \lambda_{N^c} = 1, \\
(m_L^2)_{11} &= 1347.203^2\text{GeV}^2, \quad (m_L^2)_{22} = 1238.028^2\text{GeV}^2, \quad (m_L^2)_{33} = 1464.3458^2\text{GeV}^2, \\
(m_R^2) &= \delta_{ij}\text{TeV}^2, \quad (A_l) = -3\delta_{ij}\text{TeV}, \quad (A'_l) = 3\delta_{ij}\text{TeV}, \quad A_{N^c} = A_N = 2\delta_{ij}\text{TeV}, \\
m_{\tilde{e}_L^1} &= 3250\text{GeV}, \quad m_{\tilde{e}_L^2} = 3250\text{GeV}, \quad m_{\tilde{e}_L^3} = 3260\text{GeV}, \quad m_{\tilde{e}_R^1} = 3600\text{GeV}, \\
m_{\tilde{e}_R^2} &= 3400\text{GeV}, \quad m_{\tilde{e}_R^3} = 3200\text{GeV}, \quad m_{\tilde{\nu}_L^i} = m_{\tilde{\nu}_R^i} = 2\text{TeV}, \quad m_{H_d^2} = 1\text{TeV}, \\
B_L &= 1\text{TeV}, \quad \tan \beta = 10, \quad \tan \beta_L = 2, \quad v_{L_t} = 3\text{TeV}, \quad (m_N^2) = \delta_{ij}\text{TeV}^2, \\
\mu_L &= 3\text{TeV}, \quad m_L = 2\text{TeV}, \quad m_{\varphi_L^0} = 1\text{TeV}, \quad m_{\bar{P}_L^0} = 1\text{TeV}, \quad g_L = 1/6.
\end{aligned} \tag{32}$$

### A. NO spectrum

At first we study the NO spectrum with the supposition for neutrino Yukawa couplings

$$\begin{aligned}
(Y_\nu)^{11} &= 1.295656092 \times 10^{-6}, \quad (Y_\nu)^{22} = 1.595819186 \times 10^{-6}, \\
(Y_\nu)^{33} &= 1.696349655 \times 10^{-6}, \quad (Y_\nu)^{12} = 9.774376457 \times 10^{-8},
\end{aligned}$$

$$(Y_\nu)^{13} = 6.418350381 \times 10^{-8}, \quad (Y_\nu)^{23} = 4.056255181 \times 10^{-8}, \quad (33)$$

and issue the numerical results for light neutrino masses and mixing angles

$$\begin{aligned} |\Delta m_A^2| &= 2.4707 \times 10^{-3} \text{eV}^2, & \Delta m_\odot^2 &= 7.5344 \times 10^{-5} \text{eV}^2, \\ \sin^2 \theta_{12} &= 0.3221, & \sin^2 \theta_{13} &= 0.0247, & \sin^2 \theta_{23} &= 0.5240, \\ m_{\nu_1} &= 1.9503 \times 10^{-1} \text{eV}, & m_{\nu_2} &= 1.9522 \times 10^{-1} \text{eV}, & m_{\nu_3} &= 2.0126 \times 10^{-1} \text{eV}. \end{aligned} \quad (34)$$

The diagrams are plotted near this point that satisfies the experiment constraints for light neutrinos.

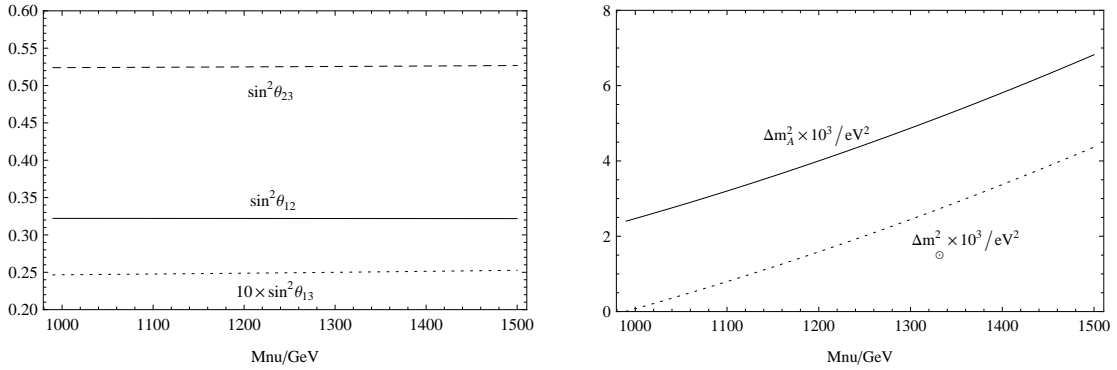


FIG. 1: With NO assumption for neutrino mass spectrum, we plot the neutrino mixing angles and mass squared differences versus  $M\nu$ . In the left diagram  $\sin^2 \theta_{12}$  (solid line),  $\sin^2 \theta_{13}$  (dotted line) and  $\sin^2 \theta_{23}$  (dashed line) versus  $M\nu$ , and in the right diagram  $\Delta m_A^2$  (solid line) and  $\Delta m_\odot^2$  (dotted line) versus  $M\nu$ , respectively.

The parameters  $(m_N^2)$  are relevant to the masses of right-handed scalar neutrinos which give contributions to neutrino mass matrix through the coupling of neutrino-sneutrino-lepton neutralino. Using the assumption  $(m_N^2) = M\nu^2 \delta_{ij}$ , we discuss how the scalar neutrinos affect the results from  $(m_N^2)$  in the Fig.1. In the left diagram of Fig.1, the neutrino mixing angles  $\sin^2 \theta_{12}$ ,  $10 \times \sin^2 \theta_{13}$  and  $\sin^2 \theta_{23}$  are represented by the solid line, dotted line and dashed line respectively. These three lines all vary weakly versus  $M\nu$  in the region  $1000 \sim 1500$  GeV. The values of  $\sin^2 \theta_{12}$  and  $\sin^2 \theta_{23}$  are around 0.32 and 0.52 respectively.  $\sin^2 \theta_{13}$  is the smallest one and near 0.025. In this region of  $M\nu$ , the three mixing angles are all satisfy the experiment bounds. We show the theoretical predictions for  $\Delta m_A^2$  and  $\Delta m_\odot^2$  versus  $M\nu$  by the solid line and dotted line in the right diagram of Fig.1. They are both

obviously increasing functions of the  $Mnu$  from 1000 GeV to 1500 GeV. Considering the experiment bounds of  $\Delta m_A^2$  and  $\Delta m_\odot^2$ , the applicable range of  $Mnu$  is near 1000 GeV.

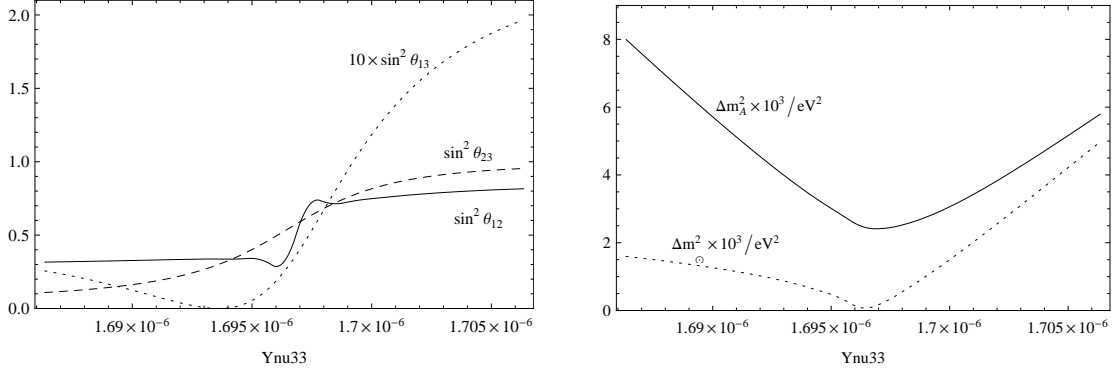


FIG. 2: With NO assumption for neutrino mass spectrum, we plot the neutrino mixing angles and mass squared differences versus  $Ynu33$ . In the left diagram  $\sin^2 \theta_{12}$  (solid line),  $\sin^2 \theta_{13}$  (dotted line) and  $\sin^2 \theta_{23}$  (dashed line) versus  $Ynu33$ , and in the right diagram  $\Delta m_A^2$  (solid line) and  $\Delta m_\odot^2$  (dotted line) versus  $Ynu33$ , respectively.

Though the neutrino Yukawa couplings are tiny, they can give important contributions to the neutrino mixing angles and masses, because they contribute at tree level. Here we discuss the effects from  $(Y_\nu)^{33}$  with the definition  $(Y_\nu)^{33} = Ynu33$ . When  $Ynu33$  varies from  $1.686 \times 10^{-6}$  to  $1.706 \times 10^{-6}$ , the behaviors of  $\sin^2 \theta_{12}$ ,  $\sin^2 \theta_{13}$  and  $\sin^2 \theta_{23}$  are studied numerically in the left diagram of Fig.2. The solid line represents  $\sin^2 \theta_{12}$ , and changes softly except the region  $(1.695 \sim 1.699) \times 10^{-6}$ . The values of  $\sin^2 \theta_{23}$  denoted by the dashed line are the increasing functions of  $Ynu33$ , and vary from 0.1 to 0.95. The dotted line represents  $10 \times \sin^2 \theta_{13}$ , which is very tiny near the point  $Ynu33 = 1.694 \times 10^{-6}$ . For the three mixing angles, the suitable region of  $Ynu33$  is near  $1.696 \times 10^{-6}$ . The right diagram in Fig.2 shows the behaviors of  $\Delta m_A^2$  (solid line) and  $\Delta m_\odot^2$  (dotted line) versus  $Ynu33$ . The values of  $\Delta m_A^2$  and  $\Delta m_\odot^2$  arrive at small numerical results as  $Ynu33$  between  $1.696 \times 10^{-6}$  and  $1.697 \times 10^{-6}$ .

Besides the diagonal elements of  $Y_\nu$ , the non-diagonal elements of  $Y_\nu$  are also important parameters. Here, we discuss how  $(Y_\nu)^{13} = Ynu13$  influences the theoretical predictions on the neutrino mixing angles and mass squared differences in the Fig.3. In the left diagram, the solid line ( $\sin^2 \theta_{12}$ ) looks like "U" in the  $Ynu13$  region  $(6.2 \times 10^{-8} \sim 6.9 \times 10^{-8})$ , and in the other regions the values of  $\sin^2 \theta_{12}$  are about 0.75 and relatively stable. The dashed line denoting  $\sin^2 \theta_{23}$  is the decreasing function of the increasing  $Ynu13$  during the region

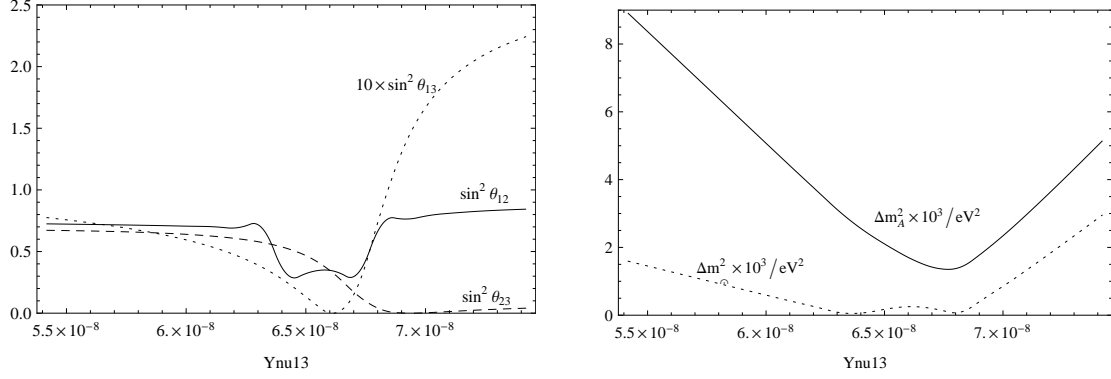


FIG. 3: With NO assumption for neutrino mass spectrum, we plot the neutrino mixing angles and mass squared differences versus  $Y_{\nu 13}$ . In the left diagram  $\sin^2 \theta_{12}$  (solid line),  $\sin^2 \theta_{13}$  (dotted line) and  $\sin^2 \theta_{23}$  (dashed line) versus  $Y_{\nu 13}$ , and in the right diagram  $\Delta m_A^2$  (solid line) and  $\Delta m_\odot^2$  (dotted line) versus  $Y_{\nu 13}$ , respectively.

( $5.4 \times 10^{-8} \sim 7.4 \times 10^{-8}$ ). We show the values for  $10 \times \sin^2 \theta_{13}$  by the dotted line which varies from almost zero to 2.25. Near the point  $Y_{\nu 13} = 6.6 \times 10^{-8}$ , the values of  $10 \times \sin^2 \theta_{13}$  are very small. In the right diagram of Fig.3, the dotted line ( $\Delta m_\odot^2$ ) is small in the range  $6.4 \times 10^{-8} < Y_{\nu 13} < 6.9 \times 10^{-8}$ . The values of  $\Delta m_A^2 \times 10^3 / \text{eV}^2$  represented by the solid line vary from 2.5 to 8.0. Taking into account the neutrino experiment bounds, the appropriate  $Y_{\nu 13}$  value is around  $6.4 \times 10^{-8}$ .

## B. IO spectrum

With the neutrino mass spectrum being IO, the neutrino mass squared differences and mixing angles are also studied numerically here. Using the following parameters

$$\begin{aligned}
 (Y_\nu)^{11} &= 1.306444732 \times 10^{-6}, & (Y_\nu)^{22} &= 1.594718138 \times 10^{-6}, \\
 (Y_\nu)^{33} &= 1.694606167 \times 10^{-6}, & (Y_\nu)^{12} &= 9.556253970 \times 10^{-8}, \\
 (Y_\nu)^{13} &= 5.940807045 \times 10^{-8}, & (Y_\nu)^{23} &= 3.061881997 \times 10^{-8},
 \end{aligned} \tag{35}$$

we get the numerical results for the neutrino masses and mixing angles at this point. The obtained numerical results are shown in the following form

$$\begin{aligned}
 \sin^2 \theta_{12} &= 0.2806, & \sin^2 \theta_{13} &= 0.0212, & \sin^2 \theta_{23} &= 0.4939, \\
 |\Delta m_A^2| &= 2.5819 \times 10^{-3} \text{eV}^2, & \Delta m_\odot^2 &= 7.6694 \times 10^{-5} \text{eV}^2,
 \end{aligned}$$

$$\begin{aligned}
m_{\nu_1} &= 1.9510 \times 10^{-1} \text{eV}, & m_{\nu_2} &= 1.9529 \times 10^{-1} \text{eV}, \\
m_{\nu_3} &= 1.8857 \times 10^{-1} \text{eV}. & & 
\end{aligned} \tag{36}$$

The light neutrino masses are all at the order of  $10^{-1}$  eV.

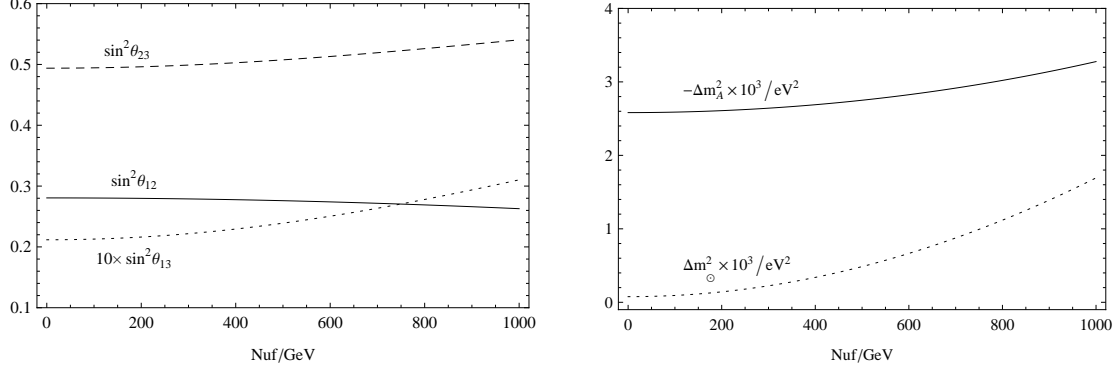


FIG. 4: With IO assumption for neutrino mass spectrum, we plot the neutrino mixing angles and mass squared differences versus  $Nuf$ . In the left diagram  $\sin^2 \theta_{12}$ (solid line),  $\sin^2 \theta_{13}$ (dotted line) and  $\sin^2 \theta_{23}$ (dashed line) versus  $Nuf$ , and in the right diagram  $-\Delta m_A^2$ (solid line) and  $\Delta m_\odot^2$ (dotted line) versus  $Nuf$ , respectively.

Here, we discuss the effects from the non-diagonal elements of  $(m_N^2)$ , and suppose  $(m_N^2)_{ij} = Nuf^2$ , for  $i, j = 1, 2, 3$  and  $i \neq j$ . In the left diagram of Fig.4, we depict the solid line( $\sin^2 \theta_{12}$ ), dotted line ( $10 \times \sin^2 \theta_{13}$ ) and dashed line( $\sin^2 \theta_{23}$ ), respectively. These three lines change mildly with  $Nuf$  varying from 0 to 1000 GeV. For the parameter  $Nuf$ , the dotted line and dashed line are both increasing functions, and the solid line is the decreasing function. The neutrino mass squared differences versus  $Nuf$  denoted by the solid line( $-\Delta m_A^2$ ) and dotted line( $\Delta m_\odot^2$ ) are plotted in the right diagram of Fig.4.  $\Delta m_\odot^2$  increases a little faster than  $-\Delta m_A^2$  with the increasing  $Nuf$ . In this parameter space,  $Nuf$  should be no more than 200GeV as shown in the Fig.4.

Here, we also discuss how the diagonal element  $(Y_\nu)^{33} = Ynu33$  influences the theoretical predictions on the neutrino mixing angles and mass squared differences in the Fig.5. From the solid line( $\sin^2 \theta_{12}$ ), dotted line( $10 \times \sin^2 \theta_{13}$ ) and dashed line( $\sin^2 \theta_{23}$ ) in the left diagram, we should take  $Ynu33$  around  $1.695 \times 10^{-6}$ . In the right diagram, both the solid line( $-\Delta m_A^2$ ) and the dotted line( $\Delta m_\odot^2$ ) reach small values near the point  $Ynu33 = 1.695 \times 10^{-6}$ . The non-diagonal element  $(Y_\nu)^{12} = Ynu12$  can obviously influence the numerical results for the neutrinos. The mixing angles( $\sin^2 \theta_{12}$ ,  $10 \times \sin^2 \theta_{13}$ ,  $\sin^2 \theta_{23}$ ) versus  $Ynu12$  are plotted by

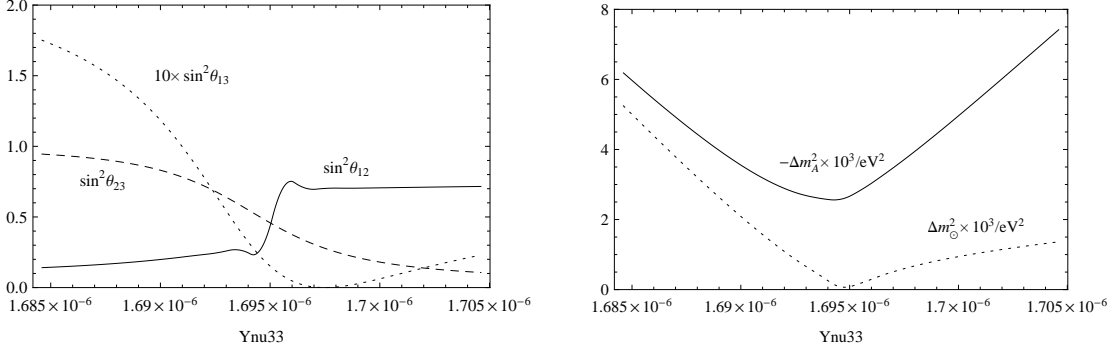


FIG. 5: With IO assumption for neutrino mass spectrum, we plot the neutrino mixing angles and mass squared differences versus  $Ynu33$ . In the left diagram  $\sin^2 \theta_{12}$  (solid line),  $\sin^2 \theta_{13}$  (dotted line) and  $\sin^2 \theta_{23}$  (dashed line) versus  $Ynu33$ , and in the right diagram  $-\Delta m_A^2$  (solid line) and  $\Delta m_\odot^2$  (dotted line) versus  $Ynu33$ , respectively.

the solid, dotted and dashed line in the left diagram of Fig.6. We show the neutrino mass squared differences  $-\Delta m_A^2$  (the solid line) and  $\Delta m_\odot^2$  (the dashed line) in the right diagram of Fig.6. From the both diagrams and neutrino experiment bounds, the appropriate value of  $Ynu12$  should be around  $9.6 \times 10^{-8}$ . As it is well known that the light neutrino masses are very tiny and there are five experiment constraints (three mixing angles and two mass squared differences), the obtained suitable parameter space is narrow.

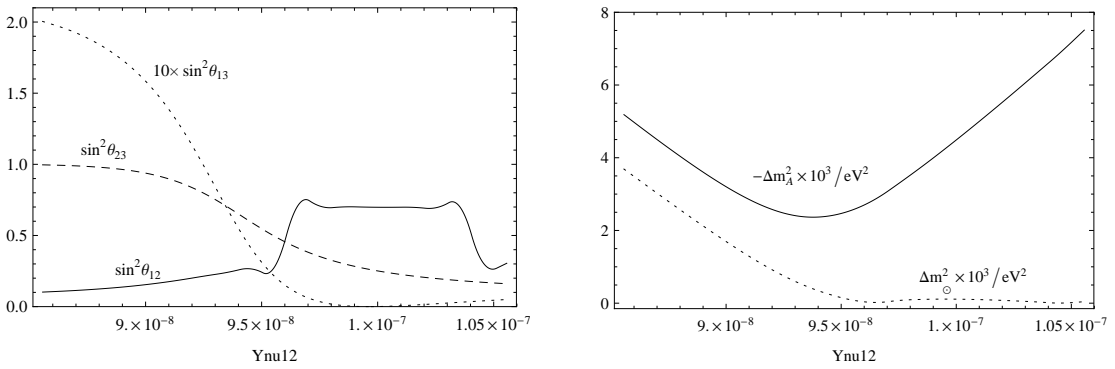


FIG. 6: With IO assumption for neutrino mass spectrum, we plot the neutrino mixing angles and mass squared differences versus  $Ynu12$ . In the left diagram  $\sin^2 \theta_{12}$  (solid line),  $\sin^2 \theta_{13}$  (dotted line) and  $\sin^2 \theta_{23}$  (dashed line) versus  $Ynu12$ , and in the right diagram  $-\Delta m_A^2$  (solid line) and  $\Delta m_\odot^2$  (dotted line) versus  $Ynu12$ , respectively.



## VI. SUMMARY

The neutrino experiment data from both solar and atmospheric neutrino experiments show that neutrinos have tiny masses and three mixing angles including two large mixing angles and one small mixing angle. The SM can not solve the neutrino experiment data, and physicists consider SM should be the low energy effective theory of a large model. So, the SM should be extended. One of the supersymmetric extensions of the SM is BLMSSM which has local gauged  $B$  and  $L$  symmetries. In this model, we have studied some processes in our previous works[13–15, 19]. In this work, with the mass insertion approximation the one loop corrections to the neutrino mixing matrix are researched.

In the BLMSSM, the tree level neutrino mass mixing matrix is obtained in our previous work[16]. The obtained one loop corrections include: 1. the virtual slepton-chargino corrections; 2. the virtual sneutrino-lepton neutralino corrections; 3. the virtual sneutrino-neutralino corrections; 4. the virtual Higgs-charged lepton corrections; 5. the exotic Higgs-neutrino corrections. We get the sum of the tree and one loop contributions to the neutrino mixing matrix. The one loop corrected effective light neutrino mass matrix  $\mathcal{M}_\nu^{eff}$  is deduced. Using the top-down method, we give the formulae for the neutrino masses and mixing angles. For neutrino mass spectrum, both NO and IO conditions are discussed numerically. In our used parameter space, the obtained numerical results for the neutrino three mixing angles and two mass squared differences can account for the corresponding experiment data. Our results imply that the light neutrino masses are at the order of  $10^{-1}$  eV.

### Acknowledgements

This work has been supported by the Major Project of NNSFC(NO.11535002) and NNSFC(NO.11275036), the Open Project Program of State Key Laboratory of Theoretical Physics, Institute of Theoretical Physics, Chinese Academy of Sciences, China (No.Y5KF131CJ1), the Natural Science Foundation of Hebei province with Grant No. A2013201277 and No. A2016201010 and the Found of Hebei province with the Grant NO. BR2-201 and the Natural Science Fund of Hebei University with Grants No. 2011JQ05 and No. 2012-242, Hebei Key Lab of Optic-Electronic Information and Materials, the midwest

universities comprehensive strength promotion project.

---

- [1] CMS collaboration, Phys. Lett. B 716 (2012) 30; ATLAS collaboration, Phys. Lett. B 716 (2012) 1.
- [2] T2K Collab., Phys. Rev. Lett. 107 (2011) 041801; MINOS Collab., Phys. Rev. Lett. 107 (2011) 181802; DOUBLE-CHOOZ Collab., Phys. Rev. Lett. 108 (2012) 131801; DAYA-BAY Collab., Phys. Rev. Lett. 108 (2012) 171803; PoS HQL 2014 (2014) 019; arXiv: 1603.03549.
- [3] M.C.G. Garcia, M. Maltonic and T. Schwetzd, arXiv:1512.06856v1.
- [4] H.P. Nilles, Phys. Rep. 110 (1984) 1; H.E. Haber and G.L. Kane, Phys. Rep. 117 (1985) 75.
- [5] J. Rosiek, Phys. Rev. D 41 (1990) 3464 [Erratum hep-ph/9511250].
- [6] M.A. Diaz, M. Hirsch, W. Porod et al., Phys. Rev. D 68 (2003) 013009; Y. Grossman, S. Rakshit, Phys. Rev. D 69 (2004) 093002; Y. Grossman and H.E. Haber, Phys. Rev. D 59 (1999) 093008.
- [7] N. Escudero, D.E.L. Fogliani, C. Munoz, et al., J. High Energy Phys. 12 (2008) 099; P. Ghosh and S. Roy, J. High Energy Phys. 04 (2009) 069; A. Bartl, M. Hirsch, S. Liebler, et al., J. High Energy Phys. 05 (2009) 120.
- [8] D.E.L. Fogliani and C. Munoz, Phys. Rev. Lett. 97 (2006) 041801; P. Bandyopadhyay, P. Ghosh and S. Roy, Phys. Rev. D 84 (2011) 115022; P. Ghosh, D.E.L. Fogliani, V.A. Mitsou, et al., Phys. Rev. D 88 (2013) 015009.
- [9] H.B. Zhang, T.F. Feng, L.N. Kou and S.M. Zhao, Int. J. Mod. Phys. A, 28 (2013) 1350117; H.B. Zhang, T.F. Feng, S.M. Zhao and T.J. Gao, Nucl. Phys. B 873 (2013) 300; H.B. Zhang, T.F. Feng, G.F. Luo, et al., J. High Energy Phys. 07 (2013) 069; H.B. Zhang, T.F. Feng, F. Sun, et al., Phys. Rev. D 89 (2014) 115007.
- [10] P. Ghosh, P. Dey, B. Mukhopadhyaya, et al., J. High Energy Phys. 05 (2010) 087.
- [11] P.F. Perez and M.B. Wise, J. High Energy Phys. 08 (2011) 068; P.F. Perez, Phys. Lett. B 711 (2012) 353; J.M. Arnold, P.F. Perez, B. Fornal, and S. Spinner, Phys. Rev. D 85 (2012) 115024; R. Barbieri and A.Masiero, Nucl. Phys. B 267 (1986) 679; S. Dimopoulos and L.J. Hall, Phys. Lett. B 207 (1988) 210.
- [12] P.F. Perez and M.B. Wise, Phys. Rev. D 82 (2010) 011901.
- [13] T.F. Feng, S.M. Zhao, H.B. Zhang, et al., Nucl. Phys. B 871 (2013) 223.

- [14] S.M. Zhao, T.F. Feng, H.B. Zhang, et al., J. High Energy Phys. 11 (2014) 119.
- [15] S.M. Zhao, T.F. Feng, B. Yan, et al., J. High Energy Phys. 10 (2013) 020; S.M. Zhao, T.F. Feng, X.J. Zhan, et al., J. High Energy Phys. 07 (2015) 124; F. Sun, T.F. Feng, S.M. Zhao, et al., Nucl. Phys. B 888 (2014) 30; S.M. Zhao, T.F. Feng, H.B. Zhang, et al., Phys. Rev. D 92 (2015) 115016.
- [16] B. Chen, S.M. Zhao, B. Yan, H.B. Zhang, T.F. Feng, Commun. Theor. Phys. 61 (2014) 619.
- [17] L.J. Hall, V.A. Kostelecky and S. Raby, Nucl. Phys. B 267 (1986) 415; F. Gabbiani, E. Gabrielli, A. Masiero and L. Silvestrini, Nucl. Phys. B 477 (1996) 321; M. Misiak, S. Pokorski and J. Rosiek, Adv. Ser. Direct. High Energy Phys. 15 (1998) 795.
- [18] B. Dziewit, S. Zajac and M. Zralek, Acta Phys. Pol. B 42 (2011) 2509.
- [19] T.F. Feng, X.Q. Li, H.B. Zhang, S.M. Zhao, arXiv:1512.06696.